Sciencia Acta Xaveriana
An International Science Journal
ISSN. 0976-1152

Volume 3
No. 1
pp. 11-25
Apr 2012

Studies on the Growth and Characterization of a new nonlinear optical Copper Guanidinium Sulphate single crystals

P. Christhuraj[1], M. Lalitha[2], S. Anbarasu[3], P.S. Joseph[4], A. Jestin Lenus[5], T. Kishore Kumar[6] and D. Prem Anand[3*]

[1] Department of Physics, St. Joseph's College (Autonomous), Tiruchirapplli - 620 002, India.
[2] Department of Physics, Jayaraj Annapackiam College for women (Autonomous), Periakulam, Theni - 625 601,India.
[3] Department of Physics, St. Xavier's College (Autonomous), Palayamkottai - 627 002, India.
[4] Department of Physics, Thanthai Hans Roever College of arts and science, Perambalur - 621 212, India.
[5] Department of Physics, College of Engineering, Anna University, Guindy, Chennai - 600 025, India.
[6] Department of Physics, Presidency College, Chennai - 600 005, India.
E-mail : dpremanand@yahoo.co.in, Phone: +91-0462-2579744

Abstract : Single crystal of semi organic nonlinear optical (NLO) material Copper Guanidinium Sulphate (CGS) of dimension 15X10X10 mm^3 was grown by slow evaporation growth technique at room temperature. Single crystal X-ray diffractometer was utilized to measure the unit cell parameters and to confirm the crystal structure. The structure of the compound was confirmed by FTIR spectral analysis. The UV-Vis-NIR result shows that the crystal has a sharp cut-off at 330 nm and is nearly 75% transparent over a wide wavelength range enabling it for optoelectronics application. The optical energy gap of CGAS was found to be 4.86 eV. The microhardness data suggest that CGS belongs to a hard material

category. The various mechanical properties fracture, toughness, brittleness context and stiffness constant were evaluated. Thermal properties of CGS crystal was investigated using TG/DTR analyses, which reveals that the material does not decomposed before melting. The resistivity and conductivity of the CGS crystal were found to be 6800 nm and 1.47 X 10^{-4} sm^{-1} respectively. The dielectric response of the sample has been studied in the frequency range 1 KHz – 10 MHz at room temperature. Kurtz powder technique confirms the second harmonic signal generation in the sample.

Key words : XRD; FTIR; Microhardness; Dielectric; NLO

1. Introduction

In the last few decades, organic materials have been of particular interest because the nonlinear optical responses in this broad class of materials is microscopic in origin, offering an opportunity to use the optical modeling coupled with synthetic flexibility to design and produce novel materials [1-2]. Hence, NLO crystals has emerged as one of the most attractive fields of current interest in view of its vital applications in areas like optical modulation, optical switching, optical logic, frequency switching and optical data storage for the developing technologies in telecommunication and in efficient signal processing [3-5]. Among the material producing NLO effects, organic and inorganic molecules possessing large second order nonlinearity finds potential applications in information storage also [6-7]. The basic structure of NLO materials is based on the π bond system due to the overlap of π - orbital delocalization of electronic charge distribution which leads to a high mobility of electron density. Functionalisation of both the ends of the Ļ-bond system with appropriate electron donor and acceptor groups can enhance the asymmetric electron distribution on either or both ground and excited states thus leading to an increased optical nonlinearity [8-12]. Hence during the last several decades, the idea of combining the inorganic distorted polyhedron with asymmetric conjugate organic molecule resulted in semiorganic materials which are attracting the great deal of attention in NLO field. Recently a new semiorganic nonlinear optical zinc guanidinium sulphate single crystal was grown and characterized [13]. Guanidine is a strong base and readily reacts with all types of organic acids to give salts with good crystallinity. The presence of size potential

donor sites for hydrogen bonding interactions and delocalized electron systems have made guanidine compounds, potentially interesting material for NLO applications [14]. In this paper, the growth of CGS single crystal from its aqueous solution by slow evaporation method followed by single crystal XRD, FTIR, UV-vis-NIR, Micro hardness, Thermal analysis, V-I characteristics, Dielectric and NLO studies have been studied and reported in detail.

2. Experimental Techniques

2.1. Synthesis

Most of the chemicals in this work were purchased from E-Merck and used without further purification. The chemicals used were carbonate (99.9% E-merck), sulphonic acid (99.9% E-merck) and copper sulphate (99.9% E-merck). Equimolar ratio of guanidine carbonate, sulphuric acid and copper sulphate were taken and dissolved in triple distilled water as per the following reactions.

$$\left[C(NH_2)_3\right]_2(CO_3) + H_2SO_4 \rightarrow \left[C(NH_2)_3\right]_2 SO_4 + H_2O + CO_2 \uparrow$$

$$\left[C(NH_2)_3\right]_2 SO_4 + CuSO_4 5H_2O \rightarrow Cu\left[C(NH_2)_3\right]_2 (SO_4)_2 + 5H_2O$$

After evaporating the water from the solution, the product CGS was obtained as a precipitate. The synthesized salt was further purified by repeated crystallization process at least thrice.

2.2. Solubility Studies

The solubility studies of CGS were carried out by measuring the amount of CGS salt that dissolved in water at 30, 35, 40, 45 and 50°C. Fig.1 shows the solubility curve of CGS in 50 mL of demonized water at different temperatures. It is seen from the solubility curve that solubility increases with increases in temperature. The synthesized salt was taken and the saturated solution was prepared in accordance with the solubility data. Seed crystals were formed by spontaneous nucleation process. Defect free, optically clear and perfectly shaped tiny crystals were chosen as seeds for the growth experiments. Good optical quality crystals of dimensions 15 X 10 X10 mm^3 (Figure 2) were grown in a period of 60-70 days.

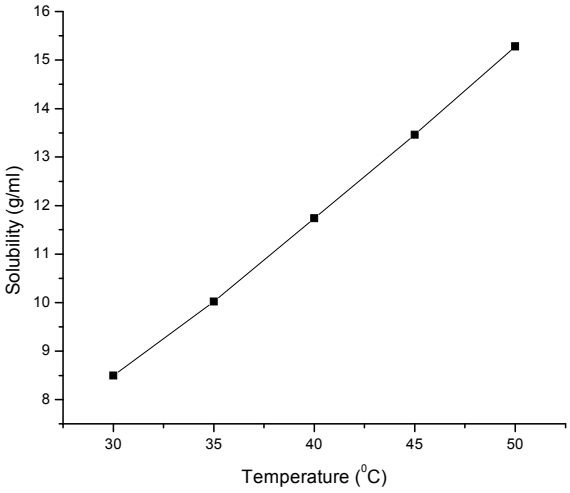

Fig. 1 Solubility Curve of CGS Single Crystal

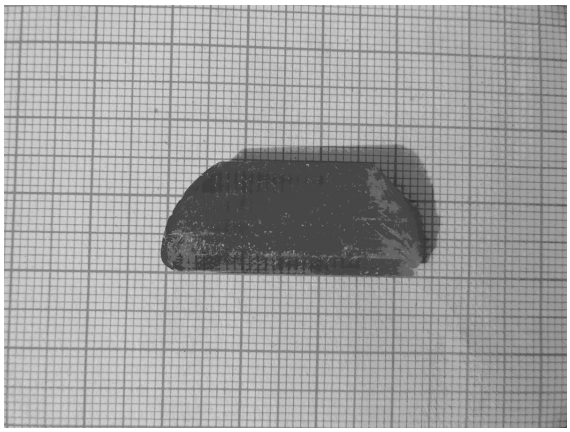

Fig. 2 Photograph of as-grown Copper Guanidinium Sulphate Single Crystal

3. Characterization Techniques

3.1. XRD Analysis

Single crystal XRD data of the as grown CGS crystals were obtained using a single crystal X-ray diffractometer (Model: ENRAF NONIUS CAD 4). The structure of CGS was solved by the direct method and refined by the least-square fit technique employing the SHELXL-97 program. It is observed that CGS is triclinic in structure with the space group P_1. Its unit cell dimensions and the interfacial angles were determined and presented in Table.1

Table.1 XRD data of CGS Single Crystal

Molecular Formula	$Cu[C(NH_2)_3]_2(SO_4)_2$
Crystal system	Triclinic
a (Å)	5.980
b (Å)	6.136
c (Å)	10.772
α (^{o})	77.28
β (^{o})	82.42
γ (^{o})	72.71
V(A^{o3})	367.2

3.2. FTIR Analysis

Fig.3 shows the FTIR spectra of CGS single crystal in the region of 4000-400 cm^{l} using the instrument BRUKER IFS-66V FTIR Spectrometer. The broad envelope below 700cm^{l} is assigned to the torsion oscillation of NH_3^+. The broad peak observed at about 3413 cm^{l} is due to N-H…O stretching band. The intense sharp peak band found at 1628 cm^{l} is due to NH_2 in plane bending modes. The band appearing in the region 1154 cm^{-1} is assigned to rocking mode of the NH_2 group. The stretching vibrations assigned to the C-S linkage occur in the region 776 cm^{-1}. A sharp intense peak at 996 cm^{l} due to the asymmetric deformation HSO^-_4 mode indicates the presence of sulphate group in the title compound. The band at 1383 cm^{-1} is assigned to C-N stretching. Thus the various functional groups in CGS molecule were identified.

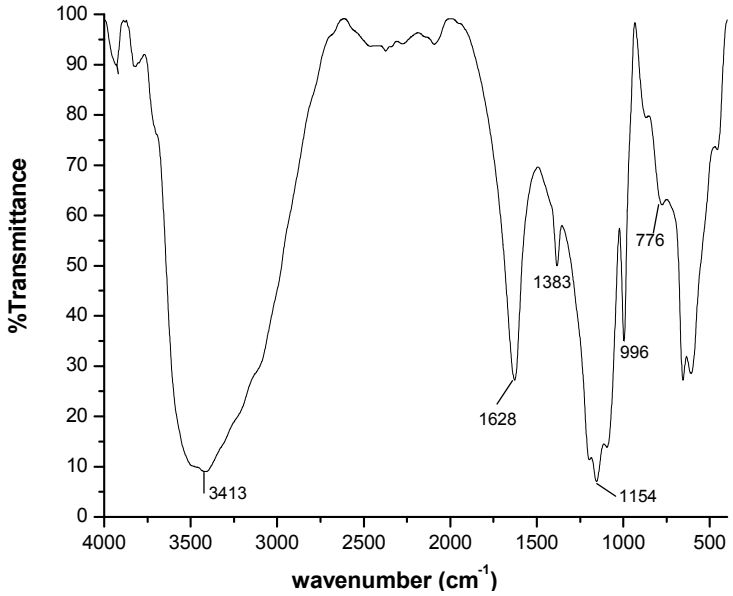

Fig. 3 FTIR Spectrum of CGS Single Crystal

3.3. UV-Vis-NIR Transmission Studies

The grown crystals of CGS were cut and polished into plates of suitable dimensions to carry out UV-Vis-NIR studies. A spectrum was recorded in the region 200-1200 nm using VARIAN CARRY 5E model UV-Vis-NIR spectrometer. The UV-Vis-NIR transmission spectrum of CGS crystal is shown in Fig.4. It is seen from the spectrum that the percentage of transmission is 10W in the wavelength range 400-700 nm. Additionally there is an abnormal absorption peak at 351 nm. The percentage of transmission is high in the wavelength range 800-1100 nm without any peaks. Hence this material may be considered as a potential candidate for optoelectronic applications with the band gap limit. The optical property of crystalline materials gives information regarding the composition nature and quality of the crystal. In a crystalline material, the region of transparency to electromagnetic radiation defines the intrinsic loss mechanism and also theoretical transmittance achievable within this region. The temporal spectral region in insulators at short wavelengths is defined by electronic transition across the band gap and at the long wavelengths by lattice vibrations [15]. The band gap of the material E_g set the limiting cut-off wavelength $\lambda_c = hc/E_g$ where h is planck's constant and c is the velocity of light. The optical band gap Eg is given by Taue's expression [16].

$$\omega^2\theta_2 = (h\omega - E_g)^2$$

where θ_2 (λ) is the imaginary part of the complex refractive index. E_g is usually derived from the plot $(\theta_2)^{1/2}$ / λ Vs $1/\lambda^2$. The intersection of the extrapolation spectrum with abscissa given the gap wavelength λ_g from which the gap energy is derived to be Eg = hc/λ_g. Alternatively energy gap is also calculated by the plot of $(\alpha h\nu)^{1/2}$ vs $h\nu$ as shown in Fig.6. The optical band gap value for CGS single crystal was good to be 4.86 eV. As a consequence of wide gap of the material, the title material is favorable for fabricating various layers of optoelectronic devices.

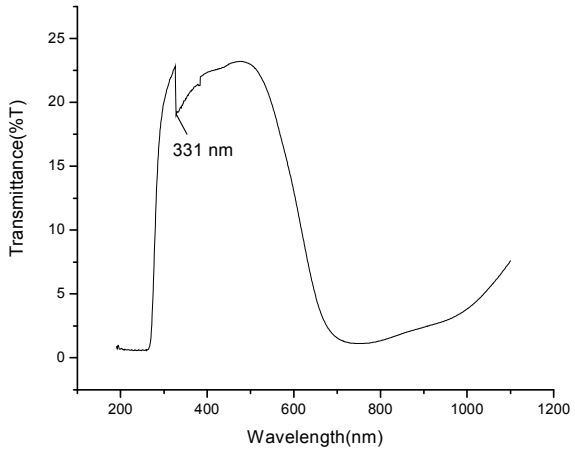

Fig. 4 UV-Vis-NIR Spectrum of CGS Single Crystal

3.4. Microhardness Studies

Micro hardness studies were carried out on CGS crystal using a Leitz Wietzlar Vickers Microhardness tester fitted with a Vickers diamond pyramidal indenter light microscope. The static indentations were made at room temperature with a constant indentation time of 15 second for all indentation. The indentation marks were made on the surfaces by varying the load from 20 to 100 g. The Vickers microhardness number H_v of the crystal was calculated using the relation $H_v = 1.8544\ P/d^2\ Kg\ mm^{-2}$, where P is the applied load and d is the average diagonal length of the indented impression in meter Vickers microhardness profile as a function of load is shown in

Fig.5. From the graph it is clear that the hardness number decreases with an increasing load. The value of work hardening coefficient (n) was estimated from the plot of log P versus load. A linear graph was observed with n value 1.35. According to Onitsch, for $1.0 \leq n \leq 1.6$, the material is regarded as hard material and $n > 1.6$ for soft materials [17].

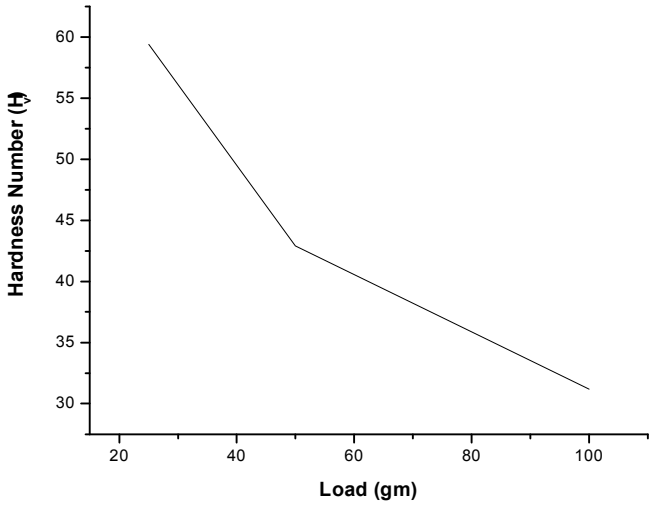

Fig. 5 Variation of Hardness Number versus Load of CGS Crystal

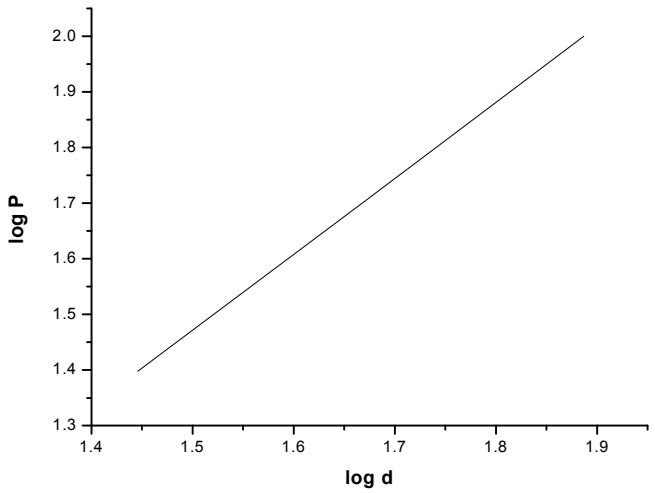

Fig. 6 Work Hardening Coefficient Curve for CGS Crystal

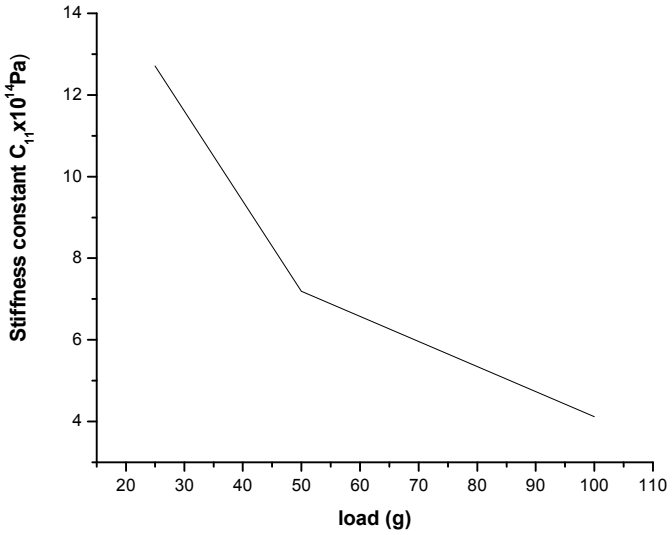

Fig. 7 Stiffness Constant Curve for CGS Crystal

The elastic stiffness constant (C_{11}) gives an idea about tightness of bonding between neighboring atoms [18]. The stiffness constants for different loads has been calculated using Wooster's empirical formula $C_{11} = H_v^{7/4}$ and is depicted in Fig. 7. From the graph it is clear that the stiffness constant decreases with increase in loads.

The toughness of the material is the resistance to fracture. The fracture toughness K_c of the material is dependent on the micro structural features and is generally insensitive to the chemical species in the surrounding environment. The expression for crack propagation under loading condition, determined by the analysis of the deformation fracture mechanics of the indentation process can be represented on the equilibrium conditions. [19]

$$P / l^{3/2} = \beta_0 K_c \qquad for \qquad l \geq d/2$$

where P is the applied load, l is the crack length measured from the centre of the indentation impression to the crack end, d is the diagonal length of the indentation impression and β_0 is the indenter constant, equal to 7 for a Vicker's diamond indenter. [20].

Brittleness is a property which affects the mechanical behavior of a material. Brittleness indices have been calculated from the ratio between the hardness, H_v and the fracture toughness K_c. The fracture toughness, the brittleness and stiffness constants for various loads are shown in Table.2

Table.2 Hardness Parameters of CGS Crystal

Load (gm)	**Fracture toughness MPa $m^{1/2}$**	**Brittleness Index $\mu m^{-1/2}$**	**Stiffness constant GPa (x 10^2)**
25	6.02874	9.8528	12.70944
50	5.60381	7.6555	7.19118
100	5.53775	5.63405	4.1188

3.5. Thermal Analysis of CGS Crystal

The thermo gravimetric analysis (TGA) and differential thermal analysis (DTA) were carried out using NETZSCH STA 409C thermal analyzer at a heating rate of 20^0C/min in the nitrogen atmosphere to determine the thermal stability of the compound between the room temperature and 375 ^{0}C. The resulting TGA/DTA trace is shown in Fig. 8. A careful examination reveals that the major exothermic peak around 79.90C which could be due to absorption of water molecules. A steady decrease in the weight observed upto 375^0C (53.37%) which may be due to the decomposition of the sample. The DTA curve shows a sharp endothermic peak at 100.72^0C which corresponds to the melting point of the compound. A very broad and sharp exothermic peak observed at 336.48^0C and 309.37^0C indicate a change in the physical state of the crystal.

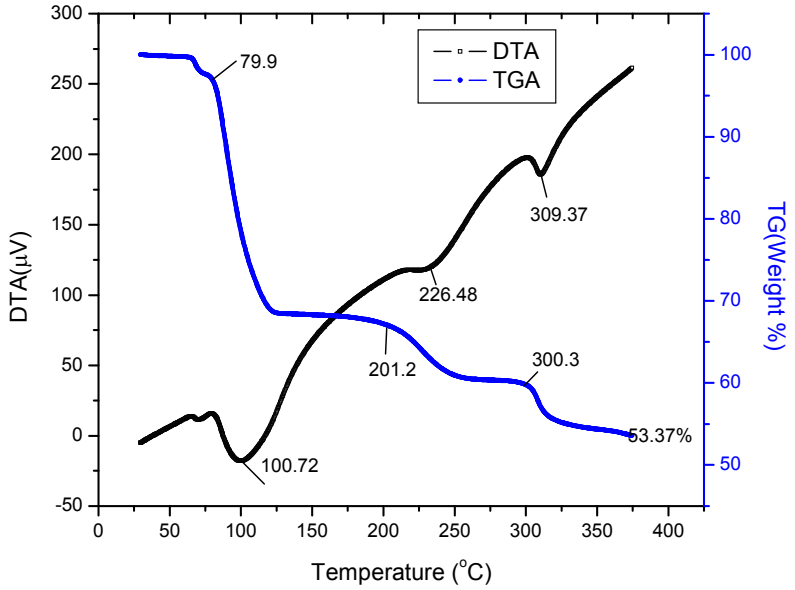

Fig. 8 TGA/DTA Curve for CGS Crystals

3.6. V-I Characteristics of CGS Crystal

The V-I characteristics of the CGS crystal at room temperature using four probe method is shown in Fig. 9. From the graph, the resistivity and the conductivity of the CGS crystal is found to be 6800Ωm and 1.47 $X10^{-4}Sm^{-1}$ respectively.

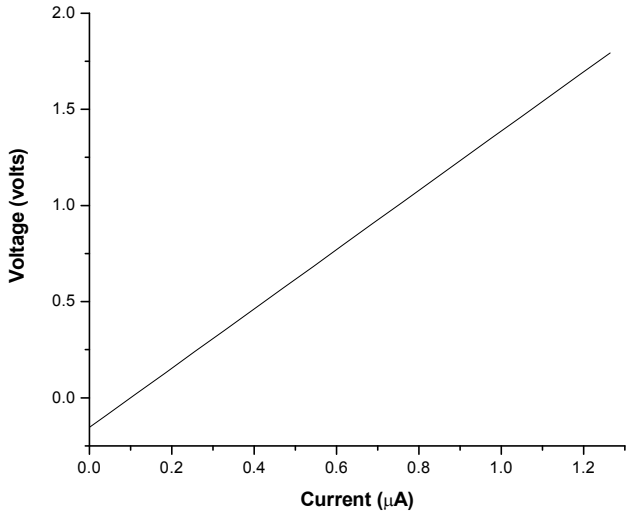

Fig. 9 V-I Characteristics of CGS Crystal

3.7. Dielectric Studies

For dielectric measurements carefully cut and polished samples of grown crystals were carried out using HIOKI 3532-50 LCR Hi TESTER in the frequency range 100 Hz to 10 MHz. A sample of crystal of dimension 4 x 3.5 x 0.5 mm^3 having silver coating on the opposite faces was placed between the two copper electrodes to form a parallel plate capacitor. Fig.10 shows the plot of dielectric constant (ε') versus applied frequency. From the graph it can be shown that the dielectric constant decreases, indicating that the grown crystals possess improved pyroelectric properties [21-22]. The dielectric loss is studied as a function of frequency for various temperatures is shown in Fig.11. These curves suggest that the dielectric loss is strongly dependent on the frequency of the applied field similar to that of the dielectric constant [23].

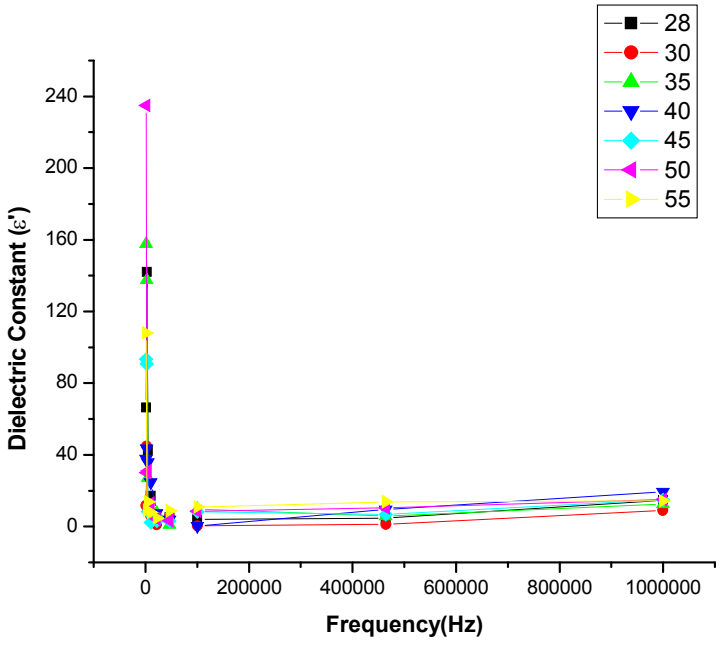

Fig. 10 Plot of Dielectric Constant (ε') versus Frequency

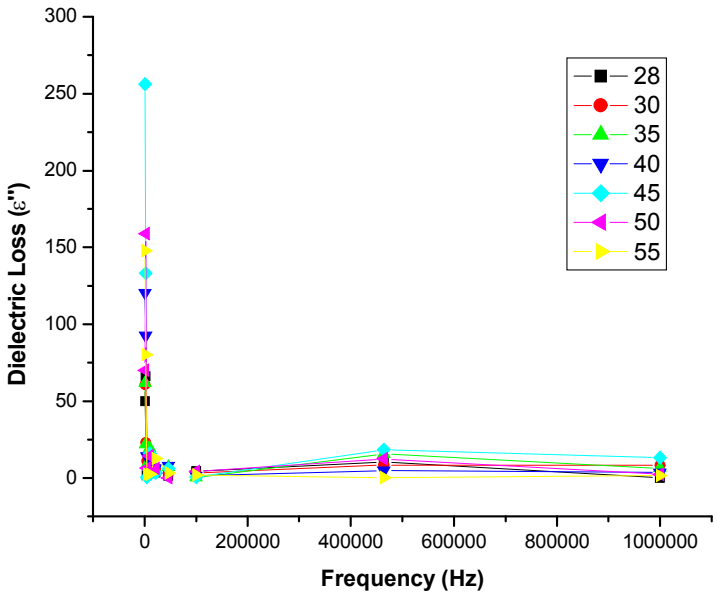

Fig. 11 Plot of Dielectric Loss (ε") versus Frequency

3.8 NLO Studies

Powder second harmonic generation (SGH) test offers the possibility of assessing the non-linearity of materials. The SHG of CGS crystal was confirmed by Kurtz SHG test. The crystal was illuminated by spectra physics Quanta-ray Nd:YAG laser using the first harmonic output of 1064 nm, with a pulse width of 8 ns. The emission of green radiation from the CGS confirms the second harmonic generation in the crystal.

4. Conclusion

A semi organic NLO material CGS was successfully grown by slow solvent evaporation technique. Single crystal XRD shows that CGS crystallizes in a noncentrosymmetric triclinic P_1 space group. The functional groups in the CGS molecule were ascertained using FTIR analysis. The band gap of CGS crystal was evaluated from UV-Vis-NIR studies. The various mechanical data were compared. E_g was from microhardness studies. Thermal studies revealed that the sample is thermally stable and has higher melting point. The conductivity and resistivity values were evaluated from V-I studies. The dielectric studies indicate that the CGS crystal possess good optical quality with lesser defects. The NLO test confirms SHG in the CGS crystalline material.

5. References

[1] P.N. Prasad, D.J. Williams, *Introduction to Nonlinear Optical Effects in Organic Molecules and Polymers* (Wiley, New York, 1991)

[2] D.S. Chemla, J. Zyss, Eds., *Nonlinear Optical Properties of Organic Molecules and Crystals* (Academic Press, Orlando, FL., 1987)

[3] H.S. Nalwa, S. Miyata, Eds., *Nonlinear Optics of Organic Molecules and Polymers* (CRC Press, Boca Raton, FL., 1997)

[4] R.A. Hann, D. Bloor, Eds., *Organic Materials for Nonlinear Optics* (The Royal Society of Chemistry, 1989)

[5] J. Badan, R. Hierle, A. Perigaud, J. Zyss, in: D.J. Williams (Ed.), *Non linear Optical Properties of Organic Molecules and Polymeric Materials*, American Chemical Symposium Series 233, (American Chemical Society, Washington, DC, 1993)

[6] P.N. Prasad, D.R. Ulrich, Eds., Nonlinear Optical and Electroactive Polymers, (Plenum Press, New York, 1988)

[7] D.R. Kanis, M.A. Ratner, T.J. Marks, Chem. Rev. **94**, 195 (1994)

[8] H.O. Marcy, M.J. Rosker, L.F. Warren, P.H. Cunningham, C.A. Thomas, L.A. DeLoach, S.P. Velsko, C.A. Ebbers, J.-H. Liao, M.G. Kanatzidis, Opt. Lett. **20,** 252 (1995)

[9] H.W. Zhang, A.K. Balra, R.B. Lal, J. Cryst. Growth **137,** 141 (1994)

[10] C.C. Frazier, M.P. Cockerham, J. Opt. Soc. Am B: Opt. Phys. **4**, 1899 (1987)

[11] Z. Li, B. Wu, G. Su, J. Cryst. Growth **178**, 539 (1997)

[12] J. Indira, P. Prakash Karat, B.K. Sarogini, J. Cryst. Growth **242**, 209 (2002)

[13] V. Siva shankara, R. Siddheswaran, T. Bharthsarathi, P.Murugakoothan, J. Cryst. Growth **311**, 2709 (2009)

[14] J. Zyss, J. Pecaut, J. P. Levy, R. Masse, Acta Crystallogr., Sect. B: Struct. Sci **49**, 334 (1993)

[15] B. Narayana Moolya, S.M. Dharmaprakash, J. Cryst. Growth **290**, 498 (2006)

[16] J. Tanc, R. Grigorovici A, Vancu, Phys. Status Solidi B,**15**, 627 (1966)

[17] Onitsch E.M, *The present status of testing the hardness of materials*, Mikroskopie, Vol.**95**, (1956)

[18] J.H. Westbrook, H. Conrad, Eds.,*The Science of Hardness Testing and Its Research Applications*, American Society for Metals (Metals Park, Ohio, 1971)

[19] B. Venkatesan, N. Kanniah, P. Ramasamy, J. Mater. Sci. Lett. **5**, 987 (1986)

[20] B.R. Lawn, D.B. Marshall, J. Am. Ceram. Soc. **62**, 347 (1979)

[21] R. Mohan kumar, R. Muralidharan, D. Rajan Babu, K.V. Rajendran, R. Jayavel, D. Jayaraman, P. Ramasamy, J. Cryst. Growth **229**, 568 (2001)

[22] Genio Su, Youping He, Hongzhi Yao, Zikong Shi, Qingjin Wu, J. Cryst. Growth **209**, 220 (2000).

[23] D. Sun, X. Yu, Q. Gu, Cryst. Res. Technol. **34**, 1255 (1999).